scientific reports

OPEN

Direct and rapid measurement of hydrogen peroxide in human blood using a microfluidic device

R. Gaikwad[1], P. R. Thangaraj[2] & A. K. Sen[1] ✉

The levels of hydrogen peroxide (H_2O_2) in human blood is of great relevance as it has emerged as an important signalling molecule in a variety of disease states. Fast and reliable measurement of H_2O_2 levels in the blood, however, continues to remain a challenge. Herein we report an automated method employing a microfluidic device for direct and rapid measurement of H_2O_2 in human blood based on laser-induced fluorescence measurement. Our study delineates the critical factors that affect measurement accuracy—we found blood cells and soluble proteins significantly alter the native H_2O_2 levels in the time interval between sample withdrawal and detection. We show that separation of blood cells and subsequent dilution of the plasma with a buffer at a ratio of 1:6 inhibits the above effect, leading to reliable measurements. We demonstrate rapid measurement of H_2O_2 in plasma in the concentration range of 0–49 μM, offering a limit of detection of 0.05 μM, a sensitivity of 0.60 $μM^{-1}$, and detection time of 15 min; the device is amenable to the real-time measurement of H_2O_2 in the patient's blood. Using the linear correlation obtained with known quantities of H_2O_2, the endogenous H_2O_2 concentration in the blood of healthy individuals is found to be in the range of 0.8–6 μM. The availability of this device at the point of care will have relevance in understanding the role of H_2O_2 in health and disease.

Reactive oxygen species (ROS), such as superoxide anion (O_2^-), hydrogen peroxide (H_2O_2), and hydroxyl radical (HO·), are free radical and reactive molecules derived from the partial reduction of molecular oxygen[1]. Cellular ROS are produced endogenously due to mitochondrial oxidative phosphorylation, or from interactions with exogenous sources such as xenobiotic compounds. Reactive oxygen species (ROS) play an essential role in regulating several signalling pathways through interaction with critical signalling molecules[2]. ROS appears as a key element in a broad range of physiological and pathophysiological processes[3] such as proliferation[4,5], metabolism, differentiation, and survival, antioxidant and anti-inflammatory response, iron homeostasis, and DNA damage response[5]. When ROS overpowers the antioxidant defence system either through an increase in ROS levels or a decrease in the cellular antioxidant capacity, oxidative stress occurs[6]. Oxidative stress results in damage to nucleic acid, proteins, and lipids[7] and can contribute to carcinogenesis[8], neurodegeneration[9], atherosclerosis, diabetes[6], and aging[10].

Hydrogen peroxide (H_2O_2) is one of the important ROS which is produced due to the incomplete reduction of oxygen in the metabolism process[11] and most cells in the human body generate H_2O_2 from superoxide[1,12]. H_2O_2 is uncharged and stable in aqueous solution and its uncharged nature helps it to diffuse and transport across the cell membrane, enabling cellular signalling away from the site of production. Moreover, H_2O_2 has a longer lifetime in comparison to other free radicals, which allows a diffusion distance up to a few milimeters[13]. H_2O_2 which is diffused out of a cell triggers cell migration, immunity generation, and cellular communication. Literature shows the usage of H_2O_2 as an intercellular and intracellular signalling molecule. For example, activated phagocytes at the site of inflammation generate H_2O_2 to control cell proliferation and platelet aggregation[7,8]. However, an imbalance in the level of H_2O_2 to the antioxidants can have a detrimental effect leading to damage of nucleic acids[13] and diseases related to oxidative stress[14]. Recently, the role of H_2O_2 in the regulation of gasotransmitters, such as nitric oxide, carbon monoxide, and hydrogen sulphide is explained[3]. Therefore, measurement of H_2O_2 level in the blood has importance in understanding the role of H_2O_2 as a potential biomarker in health and disease. Moreover, in addition to its profound significance in biological studies, H_2O_2 has relevance in other applications such as food and paper industries, environmental analysis, mineral processing, and fuel cells[15].

[1]Micro Nano Bio-Fluidics Unit, Fluid Systems Laboratory, Department of Mechanical Engineering, Indian Institute of Technology Madras, Chennai 600036, India. [2]Department of Cardiothoracic Surgery, Apollo Hospital, Chennai 600006, India. ✉email: ashis@iitm.ac.in

Blood cells including red blood cells produce H_2O_2 from multiple sources but the level of intracellular H_2O_2 is maintained as 10 nM or less due to the catalase and peroxidases[1]. The plasma H_2O_2 is mainly contributed by NOXs (nicotinamide adenine dinucleotide phosphate oxidase) on the surface of phagocytes and endothelial cells and xanthine oxidase bound to endothelial cells with a small contribution from autoxidation of small molecules. H_2O_2 can leave and enter the cells through aquaporins and the prevailing direction of H_2O_2 movement into the cells. Measurement of the concentration of H_2O_2 in the human blood has been attempted but it remains controversial since there is a large variation in the results[1]. The concentration of H_2O_2 in the human blood will depend on the dynamics of its production and its removal. It appears that the claims of steady-state plasma H_2O_2 concentration in the mid mM to high mM range was overestimated, caused by interfering factors and inadequate method and instrumentation[1]. Various compounds and contaminants present in blood plasma can react with the assaying dye leading to such overestimated values. Similarly, very low values of plasma H_2O_2 concentration ≤ 0.25 mM was also reported which could be due to the limitations of the measurement techniques[1]. The plasma H_2O_2 concentration in healthy humans appears to fall into two groups: the first group reports that the measured concentration < 10 μM and in the second group, the measured concentration is between 20 and 40μM[1]. The levels indicated by the second group is not expected for healthy individuals as H_2O_2 concentration in that range is stressful to cells, although not completely toxic. From an analysis of literature and kinetics, the most probable range for plasma H_2O_2 is 1–5 μM[1,17–20].

Various techniques for the detection of H_2O_2 have been reported, such as titration[16], spectroscopy[17], fluorescence[18], chemiluminescence[19], spectrophotometry[20], and electrochemical[21] methods. The conventional methods such as titrimetry, chemiluminescence, and spectrophotometry are not suitable because of several drawbacks such as low sensitivity, selectivity, long detection time, and complicated instrumentation involved[22]. These methods involve the manual handling of the sample, which is time-consuming and can lead to the degradation and/or change in the levels of the native hydrogen peroxide, therefore affecting the reliability of measurements. The electrochemical methods that are based on the electron transfer are preferred over the conventional methods owing to the ease of operation and integration. However, such methods have not been applied so far to the human blood sample and inherent disadvantages such as high overpotential[23] and slow electron transfer[24] leading to low sensitivity, poor selectivity, and metal fouling. Electrochemical methods based on the horseradish peroxidase (HRP) enzyme for catalytic decomposition of peroxide are more sensitive and are widely preferred[22,24]. A nanochannel platform involving HRP enzyme and carbodiimide coupling chemistry for the detection of H_2O_2 was reported[23]. In optical H_2O_2 detection, most systems involve the use of optical indicator probes. In the HRP based fluorometric assay, a colourless and non-fluorescent compound is oxidised to a fluorescent substance by hydrogen peroxide in the presence of HRP. The latter method is simple and sensitive because of the formation of a strong fluorescent product and its wide usage in a range of systems and condition[25,26]. But such methods have not been applied to human blood sample, involve manual handling and are not amenable to in-situ and continuous monitoring, which is one of the goals of the present work.

Despite the above developments in the sensor technology for the detection of H_2O_2, it is found that the concentration of measured H_2O_2 in blood spans several orders of magnitude from μM to mid mM, which can be attributed to the following: (a) there is a lack of understanding of how the concentration of H_2O_2 dynamically change between the sample collection and measurement time points, (b) most of the methods and instrumentation currently being used are inadequate to accurately measure H_2O_2 levels in the blood. Further, most of the methods reported in the literature so far are not amenable to direct and rapid measurements leading to inconsistent and delayed results. Microfluidics is a proven technology for rapid and automated measurement of a range of biomolecules[26,27]. In the present work, we address the above issues by identifying some of the critical factors that affect dynamic change in H_2O_2 in the blood plasma and develop a method based on an integrated microfluidic device for accurate and rapid measurement of exogenous H_2O_2 in blood plasma. We employ on-chip blood plasma separation to obtain cell-free plasma and dilute the plasma with a buffer to reduce the interference of blood cells and plasma proteins with H_2O_2. The device is used for measurement of the actual quantity of exogenous H_2O_2 in blood plasma to develop the correlation between FL intensity and H_2O_2 concentration. The developed correlation is then used to measure the concentration of endogenous H_2O_2 concentration in blood of healthy individuals.

Experimental

Device concept and design. The integrated microfluidic device for the detection of hydrogen peroxide (H_2O_2) in the human blood consists of three different modules (see Figs. 1a,b, S2a). In Module I, cell-free plasma is obtained by separating the plasma and blood cells from whole blood using acoustophoresis. The separated plasma from module I is then infused into module II which serves the purpose of mixing and reaction, where reagents blood plasma, exogenous H_2O_2, Amplex Red substrate and horseradish peroxidase (HRP) are mixed and incubated. In the presence of H_2O_2, the HRP oxidises the Amplex Red substrate to form resorufin which is a fluorescent compound, which is transported to module III and detected using suitable optics.

The design of the acoustics-based blood plasma separation module (Figs. 1a and S2a) is reported elsewhere[28]. The width of the main channel is 300 μm to support half-wave at a frequency of 1.91 MHz, as calculated from theory and confirmed in experiments. In the present study, the flow rate of the whole blood sample is kept constant at 20 μL min^{-1} and acoustic energy density is 14.9 J m^{-3} to obtain cell-free plasma at a flow rate of 1.0 μL min^{-1}. The function of the acoustic device is briefly described in Section S1 of "Supplementary Material". The serpentine channel for the mixing and incubation module (Figs. 1a and S2a) is designed based on diffusion coefficients of the fluids involved, flow rates, and the incubation time as follows. The experiments are performed with the assay buffer and human blood plasma and in both cases, the exogenous concentration of H_2O_2 is varied by adding the buffer to H_2O_2 stock solution of 10 μM concentration, via the mixing channel. The diffusion coefficient of liquid
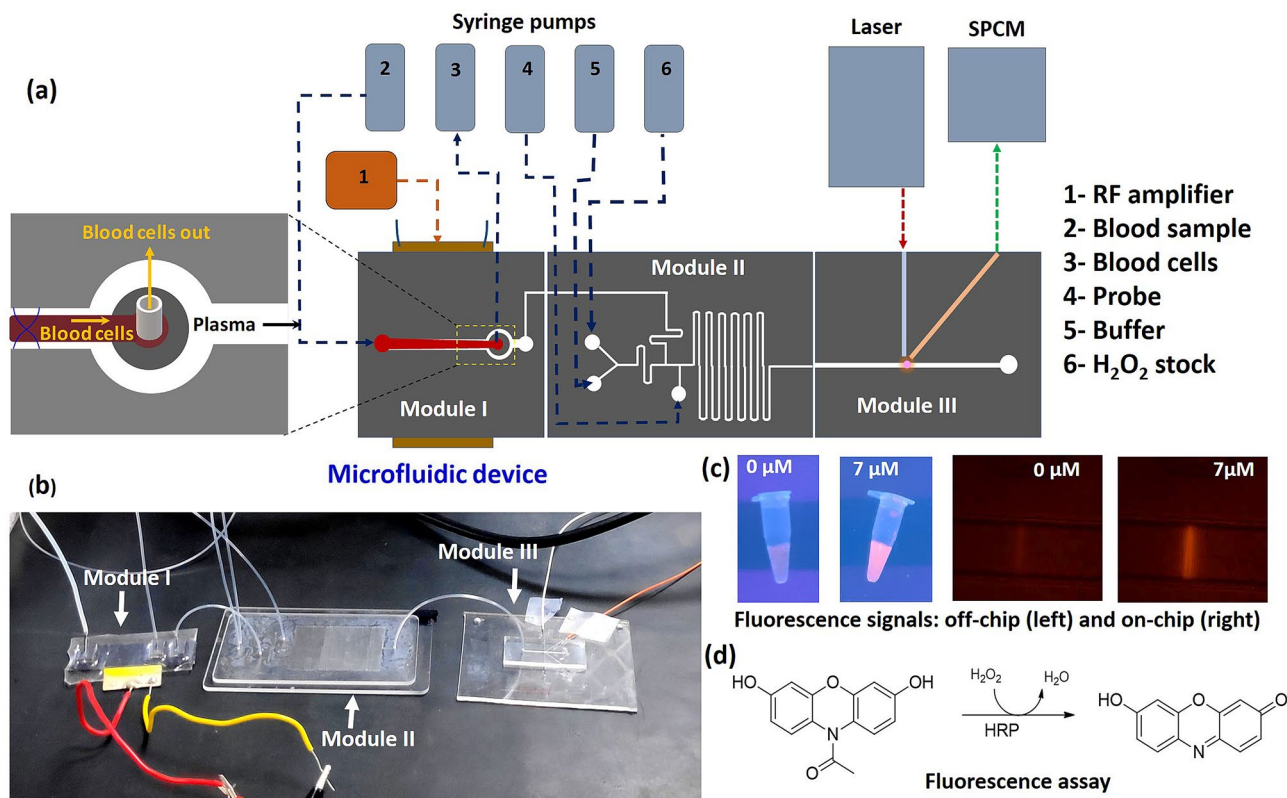
Figure 1. (**a**) Schematic of the integrated microfluidic device with the different modules (module I—blood plasma separation, module II—mixing and incubation, and module III—optical detection) and experimental setup, (**b**) photograph of the actual device showing the different modules, (**c**) Representative images showing FL signals from H_2O_2 + probe mixture in Eppendorf tube and microchannel and, (**d**) Probe chemistry.

H_2O_2 in the assay buffer is taken as[29] $D_s = 1.4 \times 10^{-5}$ cm^2 s^{-1}. The serpentine channel has a square cross-section of dimension 100×100 μm, which gives a diffusion time ($\tau = w^2/D_s$) of 7.14 s, where w is the width of the channel. In experiments with buffer, the total flow rate of H_2O_2 stock and buffer is kept constant at 3.8 μL min^{-1} while the individual flow rates are varied to obtain the different final concentrations of H_2O_2, as shown in Table S1. In experiments with centrifuged plasma, the total flow rate of H_2O_2 stock, buffer, and undiluted plasma is kept constant at 3.8 μL min^{-1}. while the flow rate of the undiluted plasma is kept fixed at 0.54 μL min^{-1} (1:6 dilution of plasma is obtained on-chip by infusing additional buffer along with H_2O_2 stock), the individual flow rates of the buffer and H_2O_2 stock is varied (with a total flow rate of 3.26 μL min^{-1}) to achieve the different final concentrations of H_2O_2 (see details in Section S2 and Table S1 in "Supplementary Material"). In experiments with on-chip separated plasma in the integrated device, the plasma flow rate is maintained at 1.0 μL min^{-1}, and the sum of the individual flow rates of the buffer and H_2O_2 stock is varied, with a total flow rate of 2.8 μL min^{-1}, to achieve the different final concentrations of H_2O_2, as shown in Table S1. The velocity (u) of the stock and buffer mixture in the channel is 6.33 mm s^{-1} and therefore the corresponding diffusion length ($L = u\tau$) is 45 mm suggesting a mixing channel of length ≥ 45 mm. Next, the probe (HRP + Amplex Red substrate) is infused into the channel at a flow rate of 0.2 μL min^{-1}, giving a total probe + H_2O_2 flow rate of 4 μL min^{-1}. Since the major constituent of the probe is the assay buffer, the probe and H_2O_2 mix quickly during incubation. The length required for mixing is taken as the length required for the incubation, to ensure the probe and H_2O_2 reaction to complete. Since the H_2O_2 assay requires a minimum incubation time of 15 min for the reaction to complete, as found later in the "Results and discussion" section, a minimum length of the serpentine channel is maintained as 6.0 m to ensure adequate mixing and incubation.

The width and depth of the fluidic channel in the optical detection module (Fig. 1a and S2a) are 100 μm and 150 μm, respectively. Two different optical fibre grooves, of width and depth 150 μm are used to incorporate the excitation fibre (10/125 μm) and FL collection fibre (62.5/125 μm). The excitation fibre groove is placed perpendicular to the flow channel and the FL collection fibre groove is placed at an angle of 45° to the excitation fibre groove to minimise the direct exposure of the detector to the excitation light coming from the laser source. A minimum gap of 50 μm is maintained between the edges of the optical grooves and the flow channel sidewalls to minimize the attenuation of the excitation and emission signals. An index matching liquid, of refractive index (RI) = 1.458, matching with the RI of fiber-glass, is filled between the edge of the fibres and the edges of the fibre grooves to prevent scattering of signals. At a total flow rate of 4 μL min^{-1} through the detection channel, the sample crosses the laser beam at a velocity of 4.4 mm s^{-1}. For a laser beam of width 40 μm in the channel, the sample residence time is 8.18 ms, which allows the signal to be easily captured by a high-speed detector.

Device fabrication and setup. Module I (blood plasma separation module) of the device is fabricated in silicon and glass substrates. Following photolithography, the channels (of 200 μm depth) are etched on a 500 μm thick silicon wafer (Semiconductor Technology and Applications, USA) using deep reactive ion etching (DRIE) technique. A borosilicate glass slide (Semiconductor Technology and Applications, USA) of 500 μm thickness is then bonded with the DRIE-etched silicon wafer by anodic bonding to seal the channels. A detailed procedure followed for the fabrication of the blood plasma separation module is reported elsewhere[28]. Module II (mixing and incubation module) and Module III (optical detection module) are machined in Polymethyl methacrylate (PMMA) using a CNC micro-milling machine (Minitech machinery, USA) as per the design outlined in the previous section. The required channel length of 6.0 m is accommodated on a PMMA sheet of size 7.5 cm × 3.5 cm. The PMMA layer with machined channels is bonded with a planar PMMA layer by first exposing both the surfaces to chloroform (≥ 99% stabilised, Ranken Chemical, India) for 2 min, by maintaining a 2 mm gap between the chloroform interface and PMMA surface, and then applying a pressure of 1.5 tons while exposing to a temperature of 65 °C for 30 min using a thermal–hydraulic press (Specac Ltd, UK). The roughness and optical transmittance of PMMA channels after machining, chloroform exposure, and heat treatment are discussed in the Supplementary Material Section S3.

A schematic and photograph of the experimental setup are shown in Fig. 1a. In on-chip blood plasma separation, the whole blood sample is infused into the device and concentrated blood cells are extracted out of the device using high-performance syringe pumps (Cetoni GmbH, Germany). For the acoustic actuation, the RF signal is generated using a function generator (SMB100A, Rohde & Schwarz, Germany), amplified using an amplifier (75A100A, Amplifier Research, USA) and the amplified signal is supplied to a lead-zirconate-titanate (PZT) transducer (Sparkler Ceramics, India) attached to the bottom of the silicon substrate using epoxy glue. The operating frequency is 1.91 MHz, and the power input is 206 mW. Depending on the experiments, different samples and reagents—buffer, H_2O_2 stock, plasma, and probe are infused into the device at the respective flow rates (Table S1). The fluidic connection between the pumps and the device inlets/outlet ports and the drain reservoir and between the different modules is established using polyethylene tubing (see Fig. 1b). A laser source (Wave Form Systems, Inc., USA) of 532 nm wavelength and 5 mW power is used as the excitation source and the fluorescence (FL) signal is detected using a single-photon counting module (SPCM) detector (50A/M, Thorlabs Inc., USA). A standard single-mode fibre (10/125 μm) carries the laser beam from the source to the channel and multimode fibre (62.5/125 μm) is used to carry the FL signal to a highly sensitive single-photon counting module (SPCM). The compound resorufin interacts with the laser beam and generates an FL signal with a peak at 590 nm. A bandpass filter (ET575/50m, Chroma Technology Corp. USA) is used to eliminate the background signal. The system involves minimal human intervention for operation and is suitable for real-time measurements.

Results and discussion

Demonstration of the assay: measurement of H_2O_2 in buffer off-chip and on-chip.
As discussed in the "Materials and methods" section, a mixture of amplex red and horseradish peroxidase (HRP) is used as the chemical probe for the detection of H_2O_2 in buffer and plasma. In the presence of amplex red, HRP reacts with H_2O_2 to produce a fluorescent (FL) compound—resorufin (Fig. 1d). The FL compound is detected by exciting it with a laser and detecting the emission signal using a photodetector, as described earlier. The representative images of fluorescence signal in the Eppendorf tube and inside a microfluidic channel are shown in Fig. S2b and Fig. 1c (see details in the Supplementary Material Section S4).

First, we perform experiments to demonstrate the FL assay and determine the minimum incubation time required, by measuring H_2O_2 in buffer using a 96-well plate. H_2O_2 stock is mixed with the buffer to achieve H_2O_2 concentration (c) in the range of 0–7 μM. The buffer containing H_2O_2 is mixed with the probe and the mixture is incubated for 15 min and FL intensity is measured using a plate reader (see Fig. S3). The relative volumes of the buffer and H_2O_2 stock solution used to achieve different concentrations of H_2O_2 is given in Table S1. Inset in Fig. S3 shows that the peak FL intensity is observed at an emission wavelength of 590 nm. The normalized FL intensity versus H_2O_2 concentration (see Fig. S3) is correlated as, $I^* = 1.04c$ (with $R^2 = 0.92$). Here a general definition of the normalized intensity $I^* = (I - I_o)/I_{en}$, where I is the FL intensity measured at a particular concentration of H_2O_2, and I_o is the FL intensity of the probe in buffer and I_{en} is the FL intensity of the endogenous H_2O_2, i.e. with only plasma and probe but without any externally added H_2O_2). For buffer experiments, I_{en} is the same as that of I_o as there is no endogenous H_2O_2 present. Inset in Fig. S3 shows that a minimum of 15 min of incubation time is required for the completion of the assay reaction since we did not observe any significant change in the FL intensity when the buffer + probe mixture is incubated for more than 15 min (see inset in Fig. S3).

Although FL based detection is possible using a 96-well plate reader, it involves manual handling of the sample, and exposure to the light and ambient and hence will lead to a faster and much higher degradation in the H_2O_2 level in the sample. On the other hand, the system presented here is a closed system, and it needs human intervention only while infusing the blood sample, which minimizes the processing time and exposure to the external environment. Therefore our system allows monitoring the H_2O_2 in real-time which is not possible using the conventional 96-well plate configuration. Further, the use of a 96-well plate would involve a manual centrifugation step to remove the blood cells for preventing interference with the optical reader whereas in the present system the plasma separation is achieved on-chip.

Next, we demonstrate the assay for the measurement of H_2O_2 using the proposed microfluidic device. For measuring the concentration of H_2O_2 in the buffer in the microfluidic device, H_2O_2 stock at a flow rate 0–2.8 μL min⁻¹ and buffer at a flow rate of 3.8–1.0 μL min⁻¹ are infused into the device to achieve H_2O_2 concentration in the range of 0–7 μM (see Table S1). In the first case, the buffer containing H_2O_2 at a flow rate of
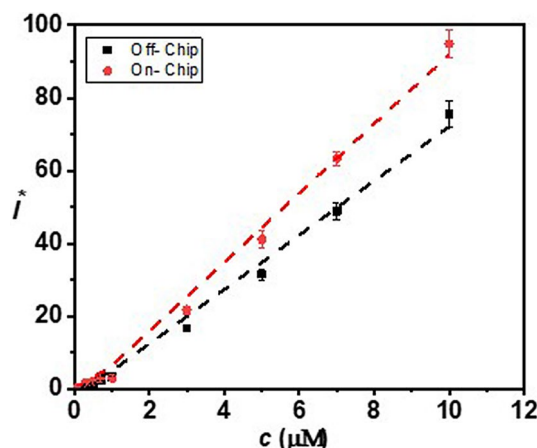
Figure 2. Variation of FL intensity with H_2O_2 concentration in buffer measured using the microfluidic device with on-chip and off-chip mixing/incubation, linear fits are obtained with $R^2 = 0.99$ and 0.98, respectively. Each data point represents the standard deviation (SD) from three different readings.

3.8 μL min^{-1} is mixed and incubated with the probe infused into the device at a fixed flow rate 0.2 μL min^{-1} in the serpentine channel for 15 min before passing to the detection module. In the second case, the H_2O_2 stock, buffer, and probe are mixed and incubated outside the device, thus allowing off-chip mixing and incubation, for 15 min and the mixture is infused into the optofluidic module at a flow rate 4 μL min^{-1}. For both cases, the variations of normalized FL intensity with concentrations of H_2O_2 is presented in Fig. 2, which show a linear trend, $I^* = Ac$, with A = 9.03 and 7.09 and $R^2 = 0.99$ and 0.98 for on-chip and off-chip mixing, respectively. The slope of the line for the off-chip mixing/incubation case is found to be smaller compared to that for the on-chip mixing case which can be attributed to the time delay of ~ 5 min between the completion of off-chip mixing/incubation and on-chip detection. For the on-chip mixing/incubation case, this time delay is ~ 500 ms, which is negligible. Further, since H_2O_2 decomposes after exposure to light and air, in the case of on-chip mixing and incubation, the mixture is minimally exposed to air and light and therefore provides an improved signal. The above experiment verifies that 15 min of incubation time is adequate for the accurate measurement of H_2O_2.

Factors affecting the measurement of H_2O_2 in blood: blood-plasma separation, deproteinization, and plasma dilution.

Next, we study the effect of blood cells and plasma proteins that alter the native as well as an exogenous concentration of H_2O_2 in blood and thus affect the measurement results and demonstrate plasma dilution as a potential solution to inhibit this effect. First exogenous H_2O_2 in blood plasma obtained via centrifugation is measured using the microfluidic device. H_2O_2 stock at a flow rate 0–2.8 μL min^{-1}, buffer at a flow rate 3.26–0.46 μL min^{-1}, and plasma at a fixed flow rate of 0.54 μL min^{-1} are infused into the device to achieve external H_2O_2 concentration (c) in the range of 0–7 μM (see Table S1). The exogenous H_2O_2 spiked plasma is then mixed and incubated with the probe infused into the device at a fixed flow rate of 0.2 μL min^{-1} in the serpentine channel for 15 min before passing into the detection module. Figure 3a shows the variation of FL intensity with the concentration of exogenous H_2O_2 in plasma. Unexpectedly, there is a fall in the FL intensity with an increase in H_2O_2 concentration initially up to c ≈ 0.4 μM (see inset of Fig. 3a) and beyond this concentration, FL intensity increases linearly with increase in concentration (with $R^2 = 0.95$). The initial decrement in the signal with an increase in the H_2O_2 concentration can be attributed to the interaction of blood cells (platelets), proteins, and other plasma constituents such as NOXs and xanthine oxidase with H_2O_2, as discussed elsewhere[1].

Here, we study the influence of blood cells and larger plasma proteins on the dynamic change of endogenous H_2O_2. We also explore the dilution of plasma to minimize the interference due to the cells, proteins, and other plasma constituents. Blood samples collected from healthy individuals at a fixed time point were centrifuged at different time points (T = 0 min, 30 min, and 60 min) allowing interaction of the endogenous H_2O_2 with the blood cells for different time durations. The plasma obtained from centrifugation of blood samples at these different time points after collection is measured at varying time points (t) after centrifugation, every 15 min. The variation of FL intensity of endogenous H_2O_2 with time is presented in Fig. 3b. It is observed that for a given centrifuged plasma sample, the FL intensity decreases with time suggesting endogenous H_2O_2 concentration in the plasma samples decreases with time. This can be because, in in-vitro condition, blood plasma does not interact with the endothelium and the tissues and therefore blood is devoid of production or the supply of H_2O_2 contributed by NOXs (nicotinamide adenine dinucleotide phosphate oxidase) on the surface of phagocytes and endothelial cells and xanthine oxidase bound to endothelial cells[1]. Further, plasma proteins act as a sink and consume H_2O_2 leading to a decrease in endogenous H_2O_2 with time. The FL intensity of plasma centrifuged at T = 0 is higher than that of plasma obtained from centrifugation of blood sample at T = 30 min and 60 min (Fig. 3b), suggesting that in the in-vitro condition the blood cells act as a sink for H_2O_2. Literature reports that blood cells including red blood cells can exchange H_2O_2 from multiple sources although the level of intracellular H_2O_2 is maintained due to the catalase and peroxidases[1]. Therefore, besides preventing interference with optical
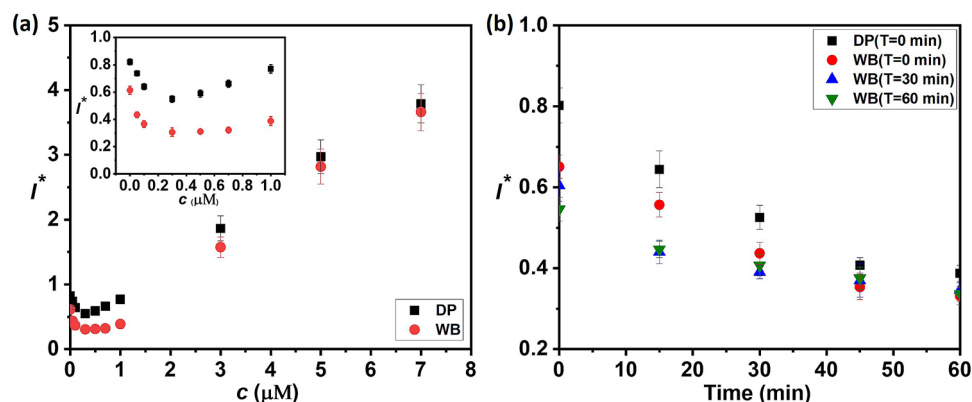
Figure 3. (**a**) Variation of FL intensity with H_2O_2 concentration measured using the microfluidic device, in human whole and deproteinized plasma. (**b**) Variation in FL intensity with measurement time points (t) for whole plasma, after the plasma gets separated at different time points (T) and deproteinized plasma (with T = 0). In all cases centrifuged plasma and on-chip mixing/incubation are used, here DP—deproteinised plasma, and WB—whole blood plasma. (Each data point represents the standard deviation (SD) from three different readings).

measurements, separation of plasma from whole blood becomes necessary to eliminate the effect of blood cells on the dynamic change of H_2O_2 for accurate measurement of H_2O_2.

To minimize the effect of plasma proteins on the consumption and therefore the dynamic change of H_2O_2, immediately after sample collection and centrifugation, the centrifuged plasma is deproteinized using a 10kD filtration column. A comparison of the FL intensity levels with time measured for whole plasma and deproteinized plasma is shown in Fig. 3b. The results show that deproteinization significantly improves the FL intensity indicating that the reaction between H_2O_2 and the probe becomes more efficient in the absence of larger proteins (> 10 kD). This can indicate that possibly larger proteins tend to quench the effect of the probe[30]. However, the FL intensity continues to decrease with time suggesting that smaller proteins (< 10 kD) contribute towards the consumption of plasma H_2O_2. A higher slope of the curve for the deproteinized plasma indicates that smaller proteins consume H_2O_2 faster leading to faster degradation in the FL intensity in the absence of larger proteins. To study the effect of exogenous H_2O_2 in deproteinized plasma, the different concentration of exogenous H_2O_2 in deproteinized plasma is measured and the variation of FL intensity with H_2O_2 concentration is shown in Fig. 3a. Although the FL intensity for deproteinized plasma is higher, in both cases, an initial decrement in FL intensity is observed up to a concentration of 0.4 μM. Therefore, although the removal of larger proteins leads to a higher FL intensity attributed to a more efficient H_2O_2 and probe reaction, the consumption of plasma H_2O_2 and consequently, the decrease in the FL intensity with time is caused by the smaller proteins. The removal of smaller proteins has been demonstrated[31] but such methods use precipitants such as Trichloroacetic acid (TCA), which can alter the native H_2O_2 concentration and therefore we do not explore such methods. Instead, we explore the dilution of plasma to minimize the interference of smaller proteins and overcome decrement in FL intensity at smaller concentrations.

We performed experiments to study the effect of plasma dilution on the reduced interaction between plasma proteins and H_2O_2. Immediately after sample collection and centrifugation (at T = 0), the centrifuged plasma is diluted with buffer at different dilutions in the range 1:1–1:10 (see flow rates in Table S3 in "Supplementary Material"). Figure 4a shows the variation of the measured FL intensity with the concentration of exogenous H_2O_2 in the diluted plasma at different dilutions. Interestingly, we see that the initial decrement in FL intensity with an increase in the exogenous H_2O_2 concentration is not observed at higher dilutions indicating that the interference due to plasma proteins and other molecules is suppressed. The results show that at a dilution of 1:6, the interference is eliminated and a linear increase in the FL intensity with the exogenous plasma concentration is observed, and $I^* = 0.67c + 0.33$ (with $R^2 = 0.98$). The inset in Fig. 4a (at $c = 3$ μM) shows that FL intensity increases with an increase in dilution due to a decrease in interference due to proteins and other elements. Since we have achieved linearity with 1:6 dilutions and there is no significant change in intensity between 1:6 and 1:10 dilutions, we proceed with 1:6 dilutions. The variation of FL intensity with H_2O_2 concentration for deproteinized plasma after removal of larger proteins (> 10 kD) and whole plasma at 1:6 dilution presented in Fig. 4b shows that deproteinization improves the FL intensity but linearity is observed in both cases. However, the implementation of on-chip deproteinization requires special techniques such as electrophoresis[32] or iso-tachophoresis[15] which complicates the device fabrication and operation. Therefore, we proceed with 1:6 dilutions that suppresses the interference due to proteins and other small molecules, in the subsequent studies.

Measurement of H_2O_2 in blood plasma using the microfluidic device. Finally, the integrated device, comprising blood plasma separation, mixing and incubation, and optical detection modules, is used to measure the actual quantities of exogenous H_2O_2 in blood plasma obtained on-chip at different concentrations and predict endogenous H_2O_2 concentration in healthy individuals. Whole blood samples collected from
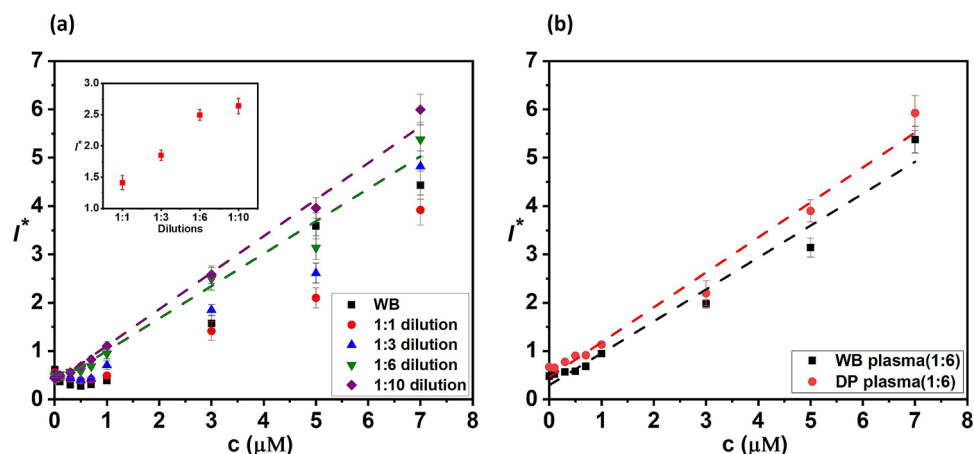
(a)

(b)

Figure 4. (**a**) Variation of FL intensity with H_2O_2 concentration in buffer-diluted whole human plasma at different dilutions, inset shows the variation of FL intensity with dilution for $c = 3$ (linear fits with $R^2 = 0.98$ for both 1:6 and 1:10 dilutions). (**b**) Variation of FL intensity with H_2O_2 concentration in buffer-diluted deproteinized and whole human plasma at 1:6 dilution (DP—deproteinised plasma, and WB—whole blood plasma). (Each data point represents the standard deviation (SD) from three different readings).
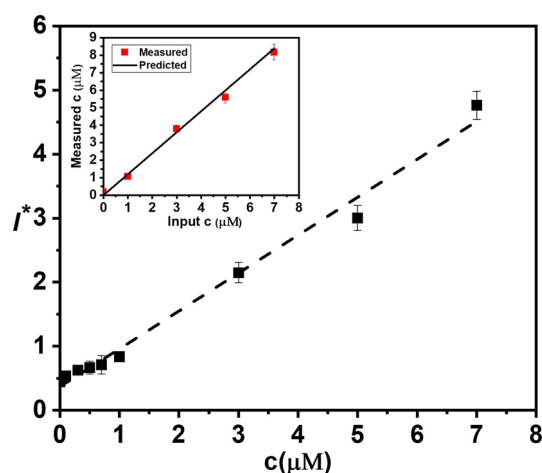

Figure 5. Variation of FL intensity with H_2O_2 concentration in human whole plasma at 1:6 dilution, measured using the integrated microfluidic device with on-chip blood plasma separation and on-chip mixing/incubation), a linear fit is obtained with $R^2 = 0.99$. Inset shows a comparison of the input H_2O_2 concentrations and predicted H_2O_2 concentrations from FL measurements, which also shows a linear fit with $R^2 = 0.98$. (Each data point represents the standard deviation (SD) from three different readings).

healthy volunteers are diluted with buffer at a 1:2 dilution ratio and infused into the microchannel at a flow rate of 20 μL min^{-1} to obtain a plasma flow rate of 1.0 μL min^{-1}. The remaining four-fold dilution of the plasma is obtained on-chip by maintaining the flow rates shown in Table S1 to achieve a final 1:6 dilution. The H_2O_2 stock at a flow rate 0–2.8 μL min^{-1}, buffer at a flow rate 2.8–0 μL min^{-1}, and plasma at a fixed flow rate of 1.0 μL min^{-1} was infused into the device to obtain exogenous H_2O_2 concentration in the range of 0–7 μM. The H_2O_2 in plasma is then mixed and incubated with the probe infused into the device at a fixed flow rate of 0.2 μL min^{-1} in the serpentine channel for 15 min before entering the detection module. The variation of FL intensity with the concentration of exogenous H_2O_2 in plasma measured using the integrated device is depicted in Fig. 5. A linear increase in the FL intensity with the plasma H_2O_2 concentration is observed, $I^* = 0.60c + 0.37$ (with $R^2 = 0.98$). The calibration obtained from the data presented in Fig. 4b is used to predict the concentration of H_2O_2 in plasma and is compared against the actual exogenous concentration of H_2O_2, as shown in the inset of Fig. 5. The curve is linear with a slope ≈ 1 and a very good match (within 2%) between the predicted and actual H_2O_2 concentration is obtained indicating that the integrated device can accurately measure the concentration of H_2O_2 in plasma. Considering the 1:6 dilution, the limit of detection of the device and assay is found to be 0.05 μM, and sensitivity is found to be 0.60 μM^{-1} (See the Section S5 in "Supplementary Material" and Fig. S4 for a zoomed view in the concentration range 0–1 μM).

Method of detection	Sensitivity	Linearity range	LOD	Response time	Sample used	Refs.
Electrochemical	39.2 µA mM^{-1} cm^{-2}	0.5 µM–50 mM	60 nM	2.0 s	Human Urine	[21]
Electrochemical	662.6 µA mM^{-1} cm^{-2}	0.3–704.8 µM	30 nM	2.0 s	Human blood serum	[22]
Electrochemical		10 nM–1 µM	10 nM		Buyer	[23]
Electrochemical	0.103 µA log(M) cm^{-2}	0.1 pM–0.1 µM	0.1 pM	6.0 s	Human blood serum	[24]
Electrochemical	1.46 nA nM^{-1} cm^{-2}	10 nM–1 µM	5 nM		Buyer	[27]
Fluorometric	0.6 µM^{-1}	50 nM–49 µM	50 nM	Instantaneous	Human blood plasma	Present work

Table 1. A compariso of the fluorometric method used here with previously reported electrochemical methods.

We collected whole blood samples from ten healthy individuals and measured the range of the values of I^*. For the exogenous H_2O_2 concentration $c = 0$, we obtained $I^* = 0.37$–0.8, which, upon considering the dilutions, predicts the endogenous concentration in the range 0.8–6 µM. A detailed comparison of the different existing methods and the present work is presented in Table 1. Most of the existing methods employ the electrochemical technique for the detection of H_2O_2. The main contribution of the present work is that we demonstrate an automated device for direct and continuous monitoring of H_2O_2 in human blood samples on-chip, and report the endogenous concentration of H_2O_2 in blood plasma. Further, most of the existing methods demonstrate H_2O_2 measurement in buffer, serum, or urine and direct measurement of H_2O_2 from the blood sample is not available. Further, externally added H_2O_2 in serum separated from blood manually is measured using the electrochemical method that involves manual steps[22,24], and measurements of endogenous H_2O_2 is not available. Also, a major disadvantage of the electrochemical method is the fouling of electrodes when used with biological samples, which reduces accuracy and sensitivity of measurement with time. Further, many electrochemical methods involved immobilisation of enzymes on the electrode surface, which can interfere with the analyte and affect the measurement. On the other hand, in optical-based detection, the sensitivity of the system remains unchanged and the device can be used over a long time without loss of accuracy or sensitivity. The only disadvantage of this system compared with electrochemical detection is the cost aspect which mainly arises because of the expensive laser and multiple syringe pumps used. But, the cost of the laser and syringe pumps can be reduced by adapting to low-cost LED sources and peristaltic pumps, respectively that could pave the way for the development of a point-of-care device. The microfluidic device and method proposed here can be used for the measurement of H_2O_2 from a minimum of 200 µL of blood within 15 min, for clinical applications. The device also holds great promise for real-time measurement of H_2O_2 in ICU patient's blood for prediction of system inflammatory syndrome (SIRS) and other medical emergency conditions[1].

Conclusions

We reported a method for direct and rapid measurement of H_2O_2 in human whole blood by employing a microfluidic device comprising a blood plasma separation module and a mixing and incubation module. The critical factors that affect the dynamics of H_2O_2 in the blood sample and therefore significantly influence the measurement accuracy was identified—it was found that the presence of blood cells and soluble proteins can significantly alter the native H_2O_2 levels in the time interval between sample withdrawal and detection. The removal of larger proteins (> 10 kDa) improved the signal but did not eliminate the interference of plasma proteins with H_2O_2, depicting the role of smaller proteins. Our study revealed that separation of blood cells and subsequent dilution of the cell-free plasma with buffer at a dilution ratio of 1:6 inhibit the interference effect. While on-chip deproteinization will require more complex techniques, on-chip blood plasma separation and dilution could be easily implemented. Our method was used to demonstrate rapid measurement of H_2O_2 in blood plasma in the concentration range of 0–49 µM, with a limit of detection of 0.05 µM, a sensitivity of 0.6 µM^{-1}, and can facilitate both discrete and real-time and continuous measurement of H_2O_2 in the patient's blood every 15 min, requiring a minimum of 300 µL of blood for discrete measurements. Using the linear correlation, $I^* = 0.60c + 0.37$ (with $R^2 > 0.98$) developed with exogenous H_2O_2, and considering dilutions, the concentration of endogenous H_2O_2 in the blood of healthy individuals was predicted to be in the range 0.8–6 µM. The measurement time of 15 min is mainly due to the time required to complete the reaction between H_2O_2 and the probe. If a fluorescence probe with a faster reaction rate is discovered in the future, and the assay can be performed in a shorter time, that will certainly reduce the measurement time. Herein, a proof of concept of a lab-scale microfluidic system has been demonstrated, that can be further developed into a point-of-care system. The system can be simplified—for example, the syringe pumps and laser can be replaced by small and cost-effective peristaltic pumps and LED sources, to develop a point of care device for use at the bedside. Our method and device can be used for accurate measurement of H_2O_2, an important signalling molecule, and an early indicator of oxidative stress. The availability of this device at the point of care will significantly help in understanding the role of H_2O_2 in health and disease.

Materials and methods

Phosphate Buffered Saline (PBS) of concentration 0.01 M and pH 7.4 is prepared by dissolving PBS (Sigma-Aldrich, USA) in DI water. Blood samples are collected from the healthy volunteers in heparin-coated vacutainers (All methods were carried out following relevant guidelines and regulations. All experimental protocols were approved by the Institute Ethics Committee, IIT Madras (Ref. No. IEC/2020/02/AK-1/01). Informed consent

was obtained from all subjects. All were adults and consented themselves). For experiments with centrifuged plasma, the collected blood sample is immediately centrifuged for 10 min at 6000 rpm and the plasma is collected (Fig. S1b). For experiments with deproteinized plasma, the plasma is centrifuged through 10 kD filtration columns (abcam, USA) at a speed of $10,000 \times g$ for 10 min to remove the proteins > 10 kD. For experiments with on-chip separated plasma, the whole blood sample diluted with PBS (1:2 dilution) is used.

Figure S2c shows that the plasma separated on-chip has higher purity, as it shows a lower absorbance compared to the centrifuged plasma. In all cases, the volume of sample blood is 200 μL, which is sufficient to maintain a continuous flow in the serpentine channel for 15 min. A mixture of amplex red substrate and horseradish peroxidase (HRP) (Fluorimetric Hydrogen Peroxide Assay Kit, Sigma Aldrich, USA) is used as the probe for the detection of H_2O_2 in buffer and plasma. The HRP catalyzes the reduction of H_2O_2 to water and in the presence of amplex red, which acts as the hydrogen donor, HRP reacts with H_2O_2 in a 1:1 stoichiometry ratio to produce resorufin, which is a fluorescent compound. First, the assay is tested via fluorescence-based measurement of H_2O_2 in the buffer in a 96-well plate reader (LS-55, Perkin Elmer Inc., USA) and subsequently using the microfluidic device. Then, externally added (exogenous) H_2O_2 at different concentrations in blood plasma obtained via centrifugation is measured using the 96-well plate reader and the microfluidic device. Further, the effect of the removal of blood cells and plasma proteins, and dilutions with buffer on the H_2O_2 measurement is studied. Finally, experiments are performed for the direct measurement of endogenous H_2O_2 in sample blood infused into the device.

The normalised fluorescence intensity is calculated using the equation, $I^* = (I - I_o)/I_{en}$, where I is the FL intensity measured at a particular exogenous concentration of H_2O_2, and I_o is the FL intensity of only the probe in buffer without any H_2O_2 and I_{en} is the FL intensity due to endogenous H_2O_2 (i.e. probe + plasma and no exogenous H_2O_2). Therefore, I^* accounts for both the endogenous and exogenous H_2O_2 concentrations. To obtain the calibration curve, we collected blood samples from three healthy individuals and extracted the plasma, and diluted the plasma with buffer at 1:6 to reduce the interference of plasma proteins on the H_2O_2 measurement. After dilution, we first measure the FL intensity corresponding to the endogenous concentration (i.e. I_{en}). Subsequently, we measure I at different exogenous concentrations of H_2O_2, and calculate the normalized FL intensity I^* at each exogenous H_2O_2 concentration, as shown in Figs. 4b and 5. In Fig. 4b, the plasma is obtained from centrifugation, and in Fig. 5, the plasma is separated on-chip using the acoustics device. Next, to determine the endogenous H_2O_2 concentration in healthy individuals, we obtained the blood samples of ten healthy individuals, separated plasma on-chip, and diluted at 1:6. We measured the endogenous FL intensity, I_{en} for each of the ten samples and used the correlation obtained from Fig. 5 and considered the dilution factor to predict the average endogenous concentration. Each data point in all the results is obtained after performing three sets of experiments and in each individual experiment, the readings are the average of five different readings.

Ethics declarations. All methods were carried out following relevant guidelines and regulations. All experimental protocols were approved by the Institute Ethics Committee, IIT Madras (Ref. No. IEC/2020/02/AK-1/01). Informed consent was obtained from all subjects or if subjects are under 18, from a parent and/or legal guardian.

Data availability
The datasets generated during and/or analysed during the current study are available from the corresponding author on reasonable request.

References
1. Forman, H. J., Bernardo, A. & Davies, K. J. A. What is the concentration of hydrogen peroxide in blood and plasma?. *Arch. Biochem. Biophys.* **603**, 48–53 (2016).
2. Watabe, S. *et al.* Highly sensitive determination of hydrogen peroxide and glucose by fluorescence correlation spectroscopy. *PLoS ONE* **6**, 1–5 (2011).
3. Mistry, R. K. & Brewer, A. C. Free Radical Biology and Medicine Redox regulation of gasotransmission in the vascular system: A focus on angiogenesis. *Free Radic. Biol. Med.* **108**, 500–516 (2017).
4. Homeostasis, O., Shadel, G. S. & Horvath, T. L. Review mitochondrial ROS signaling. *Cell* **163**, 560–569 (2015).
5. Ray, P. D., Huang, B. W. & Tsuji, Y. Reactive oxygen species (ROS) homeostasis and redox regulation in cellular signaling. *Cell. Signal.* **24**, 981–990 (2012).
6. Paravicini, T. M. & Touyz, R. M. Redox signaling in hypertension. *Cardiovasc. Res.* **71**, 247–258 (2006).
7. Halliwell, B., Clement, M. V. & Long, L. H. Hydrogen peroxide in the human body. *FEBS Lett.* **486**, 10–13 (2000).
8. Spencera, J. P. E. *et al.* DNA damage in human respiratory tract epithelial cells: Damage by gas phase cigarette smoke apparently involves attack by reactive nitrogen species in addition to oxygen radicals. *FEBS Lett.* **375**, 179–182 (1995).
9. Andersen, J. K. Oxidative stress in neurodegeneration: Cause or consequence? *Nat. Med.* **10**, S18–S25 (2004).
10. Haigis, M. C. & Yankner, B. A. Review the aging stress response. *Mol. Cell* **40**, 333–344 (2010).
11. Rezende, F., Brandes, R. P. & Schröder, K. Detection of hydrogen peroxide with fluorescent dyes. *Antioxidants Redox Signal.* **29**, 585–602 (2018).
12. Gough, D. R. & Cotter, T. G. Hydrogen peroxide: A Jekyll and Hyde signalling molecule. *Cell Death Dis.* **2**, e213–e218 (2011).
13. Zhang, K., Zheng, D.-Q., Sui, Y., Qi, L. & Petes, T. D. Genome-wide analysis of genomic alterations induced by oxidative DNA damage in yeast. *Nucleic Acids Res.* **47**, 3521–3535 (2019).
14. Kasamatsu, S. *et al.* Redox signaling regulated by cysteine persulfide and protein polysulfidation. *Molecules* **21**, 1721 (2016).
15. Mattos, I., Shiraishi, K., Braz, A. & Fernandes, J. Hydrogen peroxide: Importance and determination. *Quim. Nova* **26**, 373–380 (2003).
16. Reichert, J. S., McNeight, S. A. & Rudel, H. W. Determination of hydrogen peroxide and some related peroxygen compounds. *Ind. Eng. Chem. Anal. Ed.* **11**, 194–197 (1939).

17. Nogueira, R. F. P., Oliveira, M. C. & Paterlini, W. C. Simple and fast spectrophotometric determination of H$_2$O$_2$ in photo-fenton reactions using metavanadate. *Talanta* **66**, 86–91 (2005).
18. Gomes, A., Fernandes, E. & Lima, J. L. F. C. Fluorescence probes used for detection of reactive oxygen species. *J. Biochem. Biophys. Methods* **65**, 45–80 (2005).
19. Lee, Y. D. *et al.* Dye/peroxalate aggregated nanoparticles with enhanced and tunable chemiluminescence for biomedical imaging of hydrogen peroxide. *ACS Nano* **6**, 6759–6766 (2012).
20. Wu, C., Xia, G., Sun, J. & Song, R. Synthesis and anisotropic self-assembly of Ag nanoparticles immobilized by Pluronic F127 triblock copolymer for colorimetric detection of H$_2$O$_2$. *RSC Adv.* **5**, 97648–97657 (2015).
21. Maji, S. K., Sreejith, S., Mandal, A. K., Ma, X. & Zhao, Y. Immobilizing gold nanoparticles in mesoporous silica covered reduced graphene oxide: A hybrid material for cancer cell detection through hydrogen peroxide sensing. *ACS Appl. Mater. Interfaces* **6**, 13648–13656 (2014).
22. Thirumalraj, B., Zhao, D. H., Chen, S. M. & Palanisamy, S. Non-enzymatic amperometric detection of hydrogen peroxide in human blood serum samples using a modified silver nanowire electrode. *J. Colloid Interface Sci.* **470**, 117–122 (2016).
23. Ali, M. *et al.* Hydrogen peroxide sensing with horseradish peroxidase-modified polymer single conical nanochannels. *Anal. Chem.* **83**, 1673–1680 (2011).
24. Neal, C. J. *et al.* Picomolar detection of hydrogen peroxide using enzyme-free inorganic nanoparticle-based sensor. *Sci. Rep.* **7**, 1–10 (2017).
25. Votyakova, T. V. & Reynolds, I. J. Detection of hydrogen peroxide with Amplex Red: Interference by NADH and reduced glutathione auto-oxidation. *Arch. Biochem. Biophys.* **431**, 138–144 (2004).
26. Mishin, V., Gray, J. P., Heck, D. E., Laskin, D. L. & Laskin, J. D. Application of the Amplex red/horseradish peroxidase assay to measure hydrogen peroxide generation by recombinant microsomal enzymes. *Free Radic. Biol. Med.* **48**, 1485–1491 (2010).
27. Chikkaveeraiah, B. V., Liu, H., Mani, V., Papadimitrakopoulos, F. & Rusling, J. F. A microfluidic electrochemical device for high sensitivity biosensing: Detection of nanomolar hydrogen peroxide. *Electrochem. commun.* **11**, 819–822 (2009).
28. Karthick, S. & Sen, A. K. Improved understanding of acoustophoresis and development of an acoustofluidic device for blood plasma separation. *Phys. Rev. Appl.* **10**, 034037 (2018).
29. Tjell, A. & Almdal, K. Diffusion rate of hydrogen peroxide through water-swelled polyurethane membranes. *Sens. Bio-Sensing Res.* **21**, 35–39 (2018).
30. Yang, C. J., Jockusch, S., Vicens, M., Turro, N. J. & Tan, W. Light-switching excimer probes for rapid protein monitoring in complex biological fluids. *Proc. Natl. Acad. Sci. USA* **102**, 17278–17283 (2005).
31. Varma, S. D. & Devamanoharan, P. S. Hydrogen peroxide in human blood. *Free Radic. Res.* **14**, 125–131 (1991).
32. Goet, G., Baier, T., Hardt, S. & Sen, A. K. Isotachophoresis with emulsions. *Biomicrofluidics* **7**, 044103 (2013).

Acknowledgements

Author contributions

A.K.S. and R.G. developed the concept. R.G. performed experiments. R.G., P.R.T., and A.K.S. analyzed data, drafted and edited the manuscript. A.K.S. and P.R.T. supervised the project.

Competing interests

The authors declare no competing interests.

Additional information

Supplementary Information The online version contains supplementary material available at https://doi.org/10.1038/s41598-021-82623-4.

Correspondence and requests for materials should be addressed to A.K.S.

Reprints and permissions information is available at www.nature.com/reprints.

Publisher's note Springer Nature remains neutral with regard to jurisdictional claims in published maps and institutional affiliations.